fibers

MDPI

Article

Electrospun Nanofiber Mats with Embedded Non-Sintered TiO_2 for Dye-Sensitized Solar Cells (DSSCs)

Al Mamun [1], Marah Trabelsi [1,2], Michaela Klöcker [1], Lilia Sabantina [1], Christina Großerhode [1], Tomasz Blachowicz [3], Georg Grötsch [4], Carsten Cornelißen [4], Almuth Streitenberger [4] and Andrea Ehrmann [1,*]

1 Faculty of Engineering and Mathematics, ITES, Bielefeld University of Applied Sciences, 33619 Bielefeld, Germany
2 Ecole Nationale d'Ingénieurs de Sfax, Sfax 3038, Tunisia
3 Silesian University of Technology, Institute of Physics–Center for Science and Education, 44-100 Gliwice, Poland
4 InovisCoat GmbH, 40789 Monheim am Rhein, Germany
* Correspondence: andrea.ehrmann@fh-bielefeld.de

Received: 29 May 2019; Accepted: 1 July 2019; Published: 4 July 2019

Abstract: TiO_2 is a semiconductor that is commonly used in dye-sensitized solar cells (DSSCs). However, the necessity of sintering the TiO_2 layer is usually problematic due to the desired temperatures of typically 500 °C in cells that are prepared on polymeric or textile electrodes. This is why textile-based DSSCs often use metal fibers or metallic woven fabrics as front electrodes on which the TiO_2 is coated. Alternatively, several research groups investigate the possibilities to reduce the necessary sintering temperatures by chemical or other pre-treatments of the TiO_2. Here, we report on a simple method to avoid the sintering step by using a nanofiber mat as a matrix embedding TiO_2 nanoparticles. The TiO_2 layer can be dyed with natural dyes, resulting in a similar bathochromic shift of the UV/Vis spectrum, as it is known from sintered TiO_2 on glass substrates, which indicates an equivalent chemical bonding. Our results indicate a new possibility for producing textile-based DSSCs with TiO_2, even on textile fabrics that are not high-temperature resistant.

Keywords: TiO_2; dye-sensitized solar cell (DSSC); textile-based DSSC; electrospinning; nanofiber mat; polyacrylonitrile (PAN)

1. Introduction

Dye-sensitized solar cells (DSSCs) offer the possibility to harvest solar energy, based on non-toxic and inexpensive materials. They include a semiconducting layer for which TiO_2 is often used as a thin film or nanostructure, partly blended with other materials to increase the DSSC efficiencies [1–3]. This TiO_2 layer is coated with a monolayer of a dye, e.g., the well-known N712 or N719, including ruthenium complexes or natural dyes, often based on anthocyanins. Dyeing is necessary, since TiO_2 has a bandgap of 3.2 eV in case of the usually applied anatase modification [4] and could thus only be excited by UV light, while the applied dye must absorb most of the visible spectrum or even in the infrared to use most of the solar photons impinging on the solar cell [5]. This means that the energy distance between the lowest unoccupied molecular orbital (LUMO) and the highest occupied molecular orbital (HOMO) is necessarily much lower than the TiO_2 band gap. In addition, the LUMO energy level must be higher than the lower edge of the conduction band of TiO_2 to allow for the excited dye electrons to travel through the semiconductor. Alternatively, some research groups try

to reduce the band gap of TiO_2 by different means [6,7] or develop other semiconductors with lower band gaps [8–10] for possible application in DSSCs.

However, one problem of using TiO_2 is related to the sintering step that is necessary to fix the ceramic and to form a porous surface on which a large number of dye molecules can be adsorbed. This is why several research groups aim at finding low-temperature sintering processes.

Ji et al., e.g., report on adding a TiO_2 gel to a TiO_2 nanoparticle paste, only enabling sintering at 150 °C and resulting in an increase from 0.02% for the pure TiO_2 nanoparticle paste to 2.76% with additional TiO_2 gel [11]. Holliman et al. used colloidal TiO_2 films to reduce the sintering temperature to 120 °C [12]. Nguyen et al. investigated surface-disordered ("blue") TiO_2 for low-temperature sintering at 120 °C [13]. Diverse strategies were investigated specifically for the application on textile fabrics [14], from low-temperature sintering [15] to temperature-resistant metal wires or carbon yarns as electrodes in a textile structure [16,17].

In a former investigation by our group, we found another possibility to completely avoid the sintering step: By dip-coating a stainless steel nonwoven with fine pores into a TiO_2 solution, drying was sufficient to allow for dyeing the TiO_2 in the same way as after sintering [18,19]. However, such a stainless steel nonwoven does not reveal the typical textile properties, like a soft touch or a low bending stiffness, but behaves more like a steel sheet, despite the textile production process.

This is why we report here on investigations of a common cotton fabric as an example of a macroscopic textile and a nanofiber mat with fine pores as possible matrices to embed TiO_2 from an aqueous solution. Nanofiber mats can be produced by electrospinning [20–22], typically using water-soluble [23] or waterproof polymers [24], partly with integrated ceramics, metals, or other materials [25–27]. Polyacrylonitrile (PAN), lignin, and other materials are of special interest since they can be stabilized and carbonized after electrospinning, in this way creating conductive carbon nanofiber mats that can be used in a broad variety of applications [28–30]. Conductivity is necessary to enable the use of nanofiber mat as an electrode in a DSSC. While this property can generally be added by dip-coating a nanofiber mat in a conductive polymer [31], here the pores should be filled with TiO_2, making carbon a good choice for the nanofiber matrix under examination.

2. Materials and Methods

The spinning solution for the production of nanofiber mats contained 16% PAN that was dissolved in DMSO (min. 99.9%, purchased from S3 Chemicals, Bad Oeynhausen, Germany).

Nanofiber mats were produced on a polypropylene nonwoven as substrate while using the needleless electrospinning machine "Nanospider Lab" (Elmarco Ltd., Liberec, Czech Republic). The following spinning parameters were used for the production: high voltage 70 kV, nozzle diameter 0.8 mm, carriage speed 100 mm/s, bottom electrode/substrate distance 240 mm, ground electrode/substrate distance 50 mm, temperature in the chamber 22 °C, and relative humidity in the chamber 32%. Spinning was carried out for 30 min.

Parts of the nanofiber mats were stabilized in a muffle furnace B150 (Nabertherm, Lilienthal, Germany), approaching a typical stabilization temperature of 280 °C at a heating rate of 1 K/min, followed by isothermal treatment at this temperature for 1 h.

A furnace (Carbolite Gero, Neuhausen, Germany) was used for the carbonization process to approach a temperature of 500 °C with a heating rate of 10 K/min in a nitrogen flow of 150 mL/min (STP), followed by isothermal treatment for 1 h.

For comparison, a cotton fabric (thickness 0.19 mm, areal weight 84.49 g/m^2) was used.

For the TiO_2 solution, 15 g TiO_2 (P25 Titanium IV oxide nanopowder, 21 nm primary particle size, Sigma Aldrich, Saint Louis, MO, USA) were mixed with 125 mL distilled water and then stirred at room temperature for 15 min. Some samples (raw, stabilized, and carbonized PAN) were dip-coated into the TiO_2 solution for 5 min at room temperature and then dried.

Forest fruit tea (Mayfair, Wilken Tee GmbH, Fulda, Germany) was mixed in a ratio of 2.5 g tea:30 g distilled water for the tea solution. This tea contains anthocyanins, which are known to show

a bathochromic shift when binding to TiO_2, making the chemical binding visible by a color change with respect to the dye solution [19]. The dye was extracted for 30 min. The TiO_2-coated and TiO_2-free samples were then dyed for 30 min and then dried at room temperature. Some of the samples were rinsed with water after drying to investigate the water-fastness of the dye and the TiO_2.

The DSSCs were prepared from the TiO_2 coated carbon nanofiber mats as front electrodes and conductive plastic films containing PEDOT:PSS and graphite as counter electrodes, with non-conductive glass plates supporting both supported. The electrodes were pressed together and fixed with adhesive tape. Two drops of iodine/triiodide electrolyte (from Man Solar, Petten, The Netherlands) were added on both sides of the electrodes and spread into the cells due to capillary forces. The efficient area of the cells was 6 cm^2.

The samples were investigated by a digital microscope VHX-600D (Keyence, Neu-Isenburg, Germany), while using a nominal magnification of 200× and a scanning electron microscope (SEM) 1450VPSE (Zeiss, Oberkochen, Germany) with energy dispersive X-ray spectroscopy (EDX) for more detailed examinations of the nanofiber mat surfaces after sputtering 20 nm gold on them to avoid the charging of the samples.

The spectra of the samples were measured using a spectrophotometer sph900 (ColorLite GmbH, Katlenburg-Lindau, Germany).

Current-voltage curves of the DSSCs prepared with dyed, TiO_2 dip-coated carbon nanofiber mats were measured with a Keithley 2450 sourcemeter, while the samples were illuminated with a solar simulator LS0500 with AM 1.5 G spectrum (LOT-Quantum Design GmbH, Darmstadt, Germany).

3. Results and Discussion

Firstly, the cotton fabric and the PAN nanofiber fiber mat (without TiO_2) were dyed and dried at room temperature. Afterwards, half of the samples was rinsed with water and dried again. Figure 1 depicts some typical results.

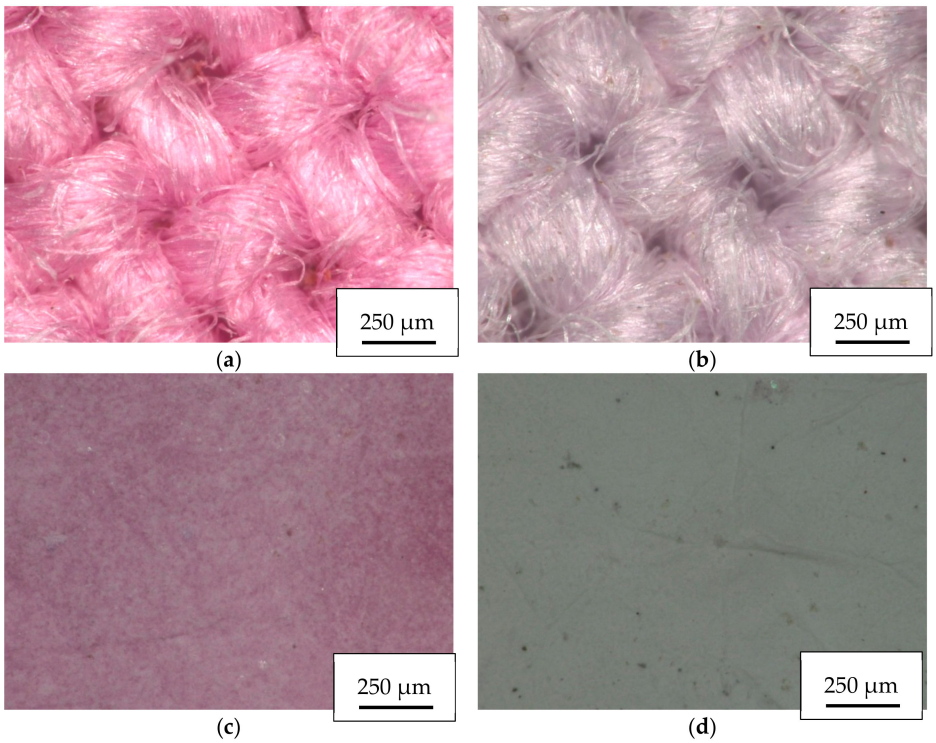

Figure 1. Microscopic images of (**a**) cotton fabric after dyeing; (**b**) cotton fabric after dyeing, drying and rinsing with water; (**c**) polyacrylonitrile (PAN) nanofiber mat after dyeing; and, (**d**) PAN nanofiber mat after dyeing, drying and rinsing with water.

After dyeing, both of the fabrics show the typical reddish color of the anthocyanins in the fruit tea. Rinsing with water reduces the color, in the case of the PAN nanofiber mat completely (Figure 1d), while the cotton fabric still shows a light reddish color (Figure 1b). Former experiments with natural dyes revealed that cotton can indeed be dyed, even without mordant [32]; however, the strong reduction of the color intensity suggests that after thorough washing not much color remains. What is more important is the finding that the raw PAN nanofiber mat does not allow the dye molecules to adhere.

Next, both of the fabrics were dip-coated in TiO_2, as described above, and afterwards dyed. Again, half of the samples were rinsed with water after the first drying step. Figure 2 depicts the results. The difference between the mostly reddish color of the TiO_2 coated cotton with some more lilac areas and the completely lilac color of the TiO_2 coated PAN nanofiber mat indicates that more TiO_2 is embedded in the nanofiber mat, while the dye molecules are not chemically bound to TiO_2 in case of cotton, but physically bound between the fibers [19]. Washing the fabrics in both cases leads to a slight blue-shift of the color, indicating that the physically bound (red) dye molecules are more strongly washed off than the chemically bound ones. Especially, on the PAN nanofiber mat, the bluish color indicates that TiO_2 is still embedded in the fabric in spite of washing. This is in strong contrast to former experiments on conductive glass or other textile fabrics on which an un-sintered TiO_2 layer could not be dyed and it was even washed off partly during dyeing [18,19].

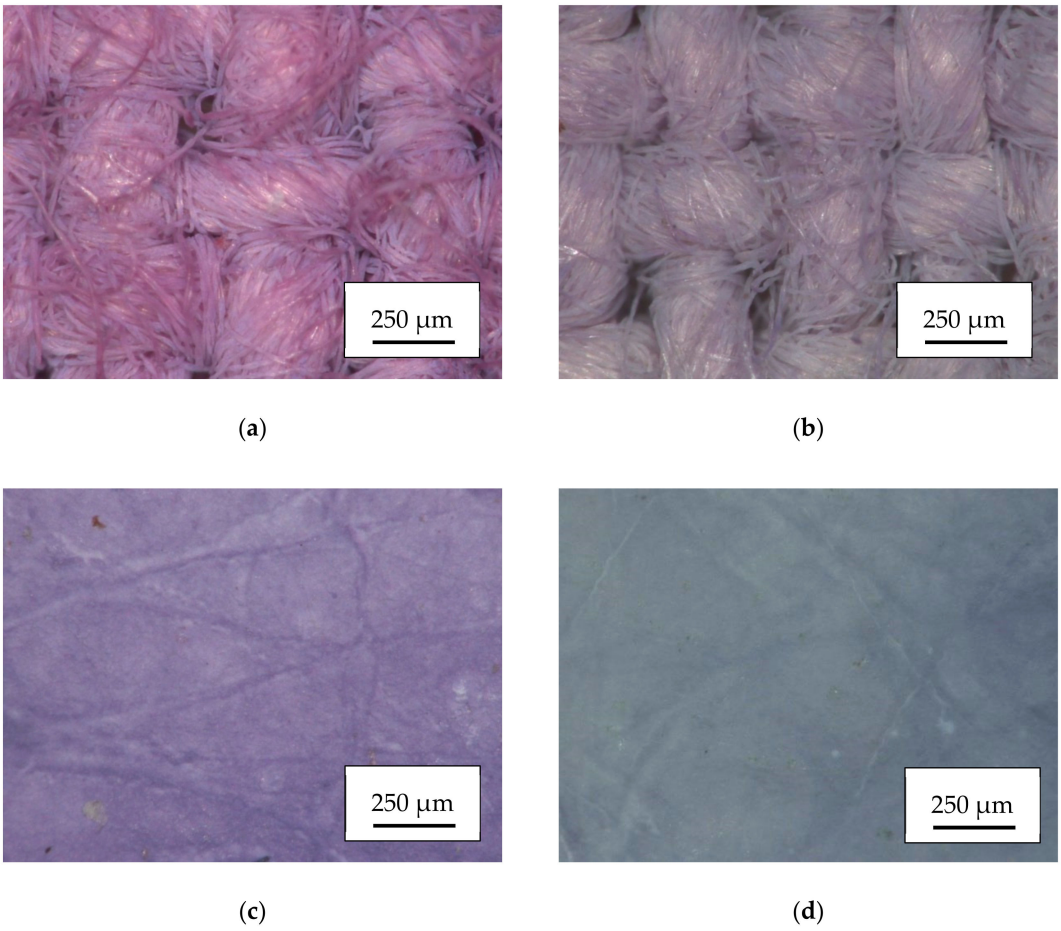

Figure 2. Microscopic images of (**a**) cotton fabric with TiO_2 after dyeing; (**b**) cotton fabric with TiO_2 after dyeing, drying and rinsing with water; (**c**) PAN nanofiber mat with TiO_2 after dyeing; and, (**d**) PAN nanofiber mat with TiO_2 after dyeing, drying, and rinsing with water.

Parts of the PAN nanofiber mats were also stabilized and carbonized at 500 °C, and afterwards dip-coated again in TiO_2 and dyed. Figure 3 depicts the results.

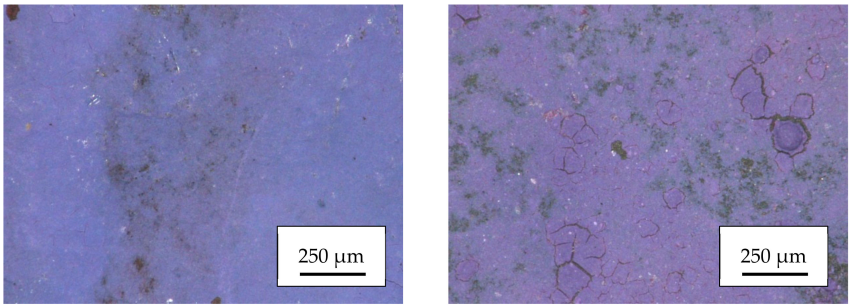

(**a**) (**b**)

Figure 3. Microscopic images of (**a**) stabilized PAN nanofiber mat with TiO_2 after dyeing; (**b**) carbonized PAN nanofiber mat with TiO_2 after dyeing.

While the color of the dyed TiO_2 on stabilized PAN (Figure 3a) is even more intense and more blueish when compared to raw PAN (Figure 2c), the TiO_2 layer on the carbonized nanofiber mat (Figure 3b) does not appear to penetrate completely into the mat, but partly stayed on top of the surface, which suggests that the dip-coating process has to be further improved for carbon nanofiber mats by modifying the coating time, the velocity at which the fabric is retracted from the TiO_2 solution, and the solid content in the solution, to avoid an unnecessary excess layer of TiO_2.

SEM images are depicted in Figure 4 for a more detailed examination of the TiO_2 layer on the nanofiber mats. On the stabilized and the carbonized PAN nanofiber mats (Figure 4c,d), a relatively even TiO_2 layer is visible, which clearly covers the nanofibers of the mat. This finding is consistent with the observation of an unnecessarily thick semiconducting layer in Figure 3b. Obviously, the TiO_2 layer should also be reduced on the stabilized PAN nanofiber mat, if this material will be used for any application. On the raw PAN nanofiber mat (Figure 4a), the nanofibers are clearly visible, embedding the TiO_2 nanoparticles. Interestingly, the surface of the PAN/TiO_2 composite looks unchanged after rinsing with water (Figure 4b), which suggests that the TiO_2 is really rigidly fixed inside the nanofiber mat.

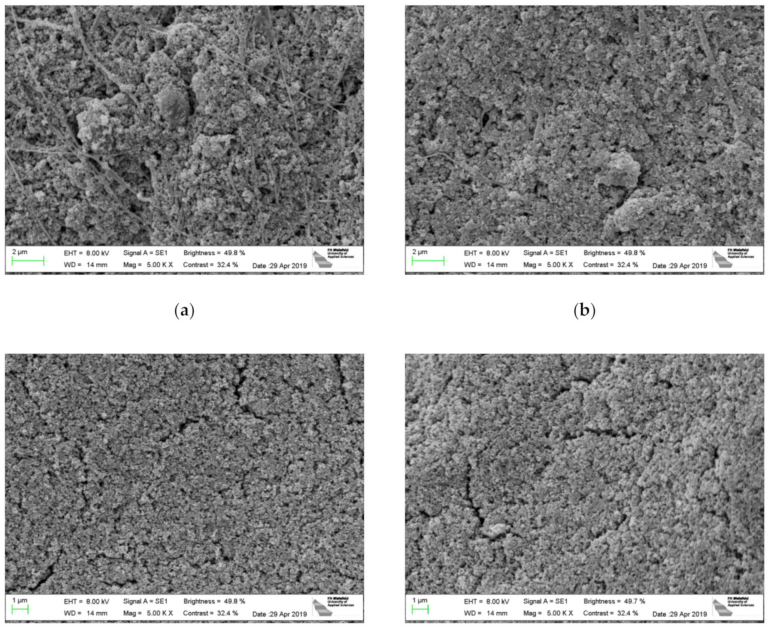

(**a**) (**b**)

(**c**) (**d**)

Figure 4. Scanning electron microscope (SEM) images of (**a**) PAN nanofiber mat with TiO_2; (**b**) PAN nanofiber mat with TiO_2 after rinsing with water; (**c**) stabilized PAN nanofiber mat with TiO_2; and, (**d**) carbonized PAN nanofiber mat with TiO_2. In all images, a nominal magnification of 5000× was used.

Figure 5 additionally underlines this, showing an SEM image of the surface after rinsing with water and dyeing, i.e., after two treatments with water. While the SEM image again shows a homogeneous distribution of the TiO_2 nanoparticles over the nanofiber mat, the EDX map does not even depict the fiber that is visible in the SEM image, revealing that the majority of the TiO_2 is stored inside the nanofiber mat.

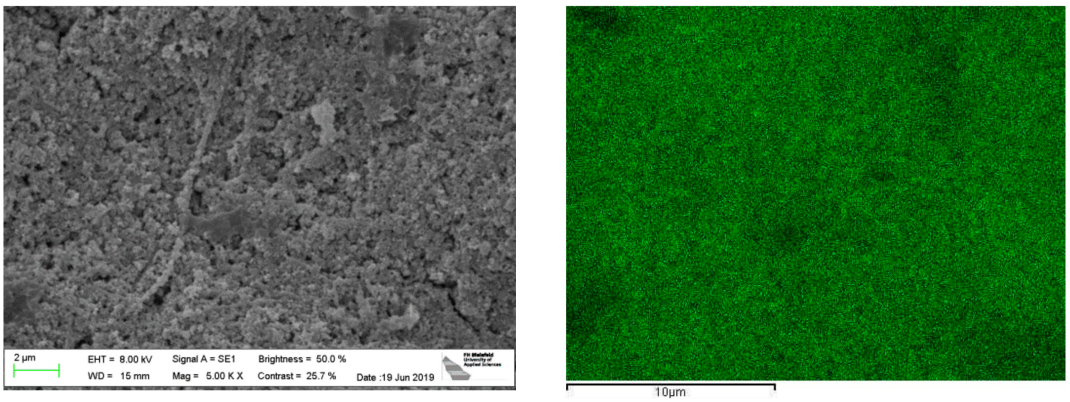

(**a**) (**b**)

Figure 5. Surface of PAN nanofiber mat with TiO_2 after rinsing with water and dyeing. (**a**) SEM image; (**b**) energy dispersive X-ray spectroscopy (EDX) map of the element Ti, taken on the identical surface spot. The fiber visible in the SEM image cannot be identified in the EDX map.

The remission spectra of the samples depicted in Figures 1 and 2 are given in Figure 6 to more quantitatively investigate the dyeing process. For the stabilized and carbonized samples, these investigations were not performed due to the changing color of the fabric itself, which is superposed on the color of the dyed TiO_2 and reduces the reliability of the corresponding spectra.

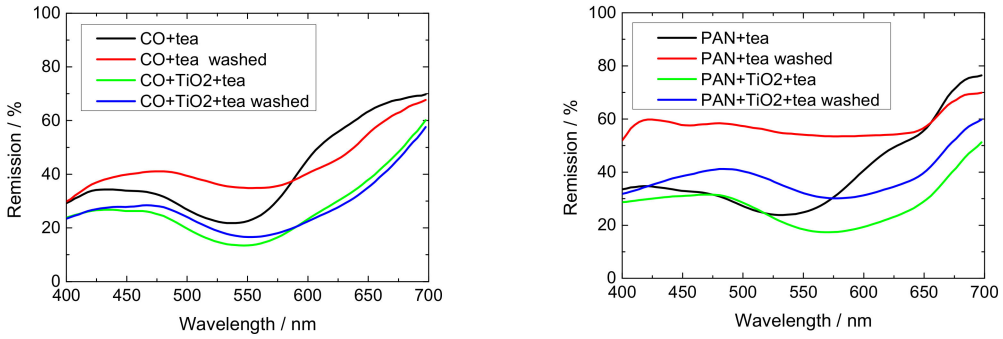

(**a**) (**b**)

Figure 6. Remission spectra of (**a**) cotton (CO); (**b**) PAN nanofiber mats with and without TiO_2 after dyeing and partly washing.

In general, the minima in the remission spectra correspond to the maxima in the correlated absorption spectra. A perfectly white fabric can be expected to show a high remission near 100% over the complete wavelength range, while a completely black one shows a remission of 0%.

When comparing the cotton and PAN fabrics dyed with tea (black lines) and washed afterwards (red lines), the fabrics become significantly lighter in both cases after washing, which indicates that the dye molecules are partly (in case of cotton) or nearly completely (in case of PAN) washed out. This is clearly different for TiO_2 dip-coated fabrics. For cotton (Figure 6a), the dyeing of the TiO_2 coated sample (green line) leads to a slight shift of the remission minimum (absorption maximum) to larger wavelengths, as expected for the desired chemical bond. A small further shift is visible after washing

this sample (blue line), indicating that the physically bound (reddish) dye molecules were washed off to a larger extent than the TiO_2 with the chemically bound (blueish) dye molecules. For PAN, the absolute increase in remission is larger, showing that more dye is washed off, which fits to Figure 2 showing the significant reduction in color intensity and which can be related to washing off excess dye that cannot be stored inside the nanofiber mat.

However, more interesting is the clearly increased bathochromic shift of the spectra measured on PAN with TiO_2, as compared to the spectra measured on cotton. This can also be recognized in Figure 7, which shows the wavelengths of the absorption maxima (equivalent to remission minima) of the spectra depicted in Figure 5. The grey rectangle indicates the wavelength range of the bathochromic shift, as measured in a former examination for TiO_2 on conductive glass with otherwise identical materials and equipment [33].

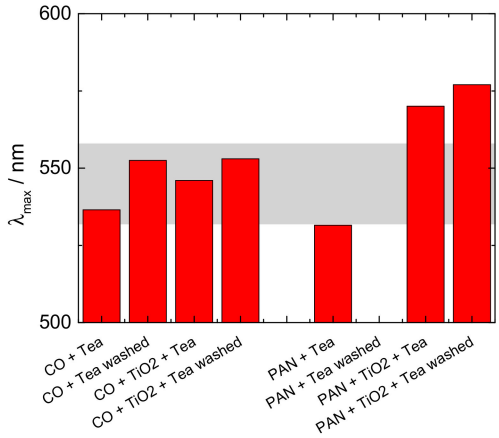

Figure 7. Wavelengths of the absorption maxima (=remission minima) of the dye spectra. No absorption maximum occurs for PAN + Tea washed.

The raw cotton and PAN show extremal wavelengths near the values that are expected at the lower border of the grey rectangle, correlated to the spectrum of the dye solution.

In all cases, the TiO_2 coating before dyeing leads to a wavelength upshift that is larger for the washed samples, since the not chemically bound dye molecules are easily washed off. On the PAN/TiO_2 nanofiber mats, this bathochromic shift is even larger than measured in the previous experiment, where a TiO_2 layer on conductive glass was dyed, suggesting a good chemical bonding of the dye to the TiO_2 in the recent experiment.

Finally, the TiO_2 dip-coated and dyed carbon nanofiber mats were introduced as front electrodes into DSSCs. Figure 8 depicts the resulting current-voltage curves.

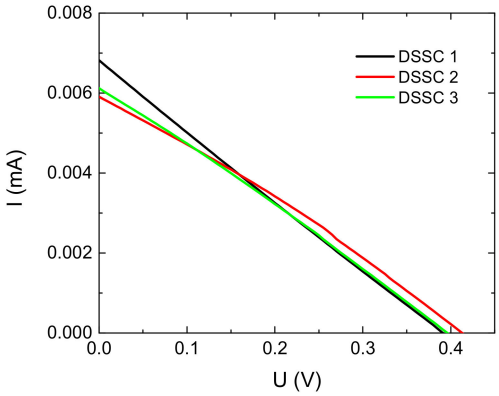

Figure 8. Current-voltage curves of dye-sensitized solar cells (DSSCs) with carbon nanofiber mats with dyed TiO_2 as front electrodes.

While the open-circuit voltages around 0.4 V are typical for anthocyanin-based dyes, the short-circuit currents that are achieved here are significantly lower than for semi-textile DSSCs with nanofiber mats as counter electrodes [31] or for DSSCs with the same foil-based counter electrodes as used here and commercially available TiO_2 coated conductive glass as front electrodes [33]. Typically efficiencies around 0.03% and 0.6% [34] are reached while using anthocyanin-based dyes without further optimization of the electrodes etc., while, in our tests we find short circuit current densities of J_{SC} ~0.001 mA/cm^2, open circuit voltages of V_{OC} ~0.4 V, fill factors of ~0.25 (identical to a straight line) and thus an efficiency of only 0.0001%, which is two to three orders of magnitude lower than the typical literature values.

This can be attributed to the relatively low carbonization temperature that results in only a low conductivity of the carbon nanofiber mat. More specifically, commercial FTO glasses that are used for DSSC experiments have typical sheet resistances of 15 Ohm, while the average sheet resistance of the carbon nanofiber mats used here was approx. 800 Ohm, i.e., by a factor of more than 50 higher. This large resistance significantly reduced the possible current flow along the carbon nanofiber mat. There are two possible paths to solve this problem in the future: On the one hand, carbonization at higher temperatures should be optimized to avoid the possible breaking of the nanofiber mats during their use in DSSCs; it is well-known from the literature that the conductivity can be strongly increased by higher carbonization temperatures. On the other hand, it is possible to add a highly conductive textile on the back of the nanofiber mat to support the in-plane conductivity.

Nevertheless, for the first general proof-of-concept as to whether nanofiber mats can be used to embed TiO_2 without a sintering step, tests with the more brittle nanofiber mats carbonized at higher temperatures, possibly leading to short circuits inside the DSSCs and thus requiring further research of the carbonization process, were avoided. Optimizing the interplay of electrospinning, carbonization, and dip-coating the nanofiber mats will be carried out in the near future.

It should be mentioned that, while only TiO_2–as one of the most interesting semiconductors in DSSC production–was tested here, this proof-of-concept should be extended to other semiconductors or generally ceramics. Especially, ZnO, which is also used in DSSCs, or $BaTiO_3$, which is interesting to be applied as a dielectric in capacitors, will be investigated in the near future. Other ceramics include Al_2O_3, which is isolating but nevertheless shows a high thermal conductivity, making a network of Al_2O_3 nanoparticles without binder interesting for heat conduction; WO_3, which can also be used in DSSCs, similar to TiO_2 and ZnO [35]; or, Nb_2O_5, which was also shown to work as a front electrode in DSSCs [36].

For these and other applications, it would be supportive to use a nanofiber mat as a matrix in which the ceramics are embedded, instead of applying them with a binder, which automatically means that they are separated from the neighboring nanoparticles, and thus destroys the possible percolation pathways. Thus, it is necessary to further investigate the possibility of using nanofiber mats as matrices for these and other ceramics and possibly further nanoparticles.

4. Conclusions

The embedding of TiO_2 in PAN nanofiber mats was found to the enable dyeing of the semiconductor without the necessity of sintering the TiO_2 layer, as it would be indispensable on glass or macroscopic textile surfaces. This allows for the use of TiO_2 on fabrics that are not heat-resistant enough to allow for sintering at the typical temperature of 500 °C.

Integration into a highly-efficient textile-based DSSC requires further optimization of the dip-coating process to avoid excess TiO_2 on the top of the carbon nanofiber mat surface and of the carbonization step to produce highly conductive, flexible carbon nanofiber mats are necessary.

Author Contributions: Conceptualization, T.B., L.S., and A.E.; formal analysis, L.S., A.E. and T.B.; investigation, A.M., M.T., M.K., L.S., C.G., G.G, C.C., and A.S.; writing—original draft preparation, L.S. and A.E.; writing—review and editing, all authors; visualization, C.G., L.S. and A.E.; supervision, L.S., A.E. and T.B.

Funding: This project was funded by Deutsche Bundesstiftung Umwelt DBU (German Federal Environmental Foundation), by the Erasmus+ program of the European Union, and by the SUT Rector Grant 14/990/RGJ18/0099.

Conflicts of Interest: The authors declare no conflict of interest. The funders had no role in the design of the study; in the collection, analyses, or interpretation of data; in the writing of the manuscript, or in the decision to publish the results.

References

1. Motlak, M.; Hamza, A.M.; Hammed, M.G.; Barakat, N.A.M. Cd-doped TiO_2 nanofibers as effective working electrode for the dye sensitized solar cells. *Mater. Lett.* **2019**, *246*, 206–209. [CrossRef]
2. Desai, N.D.; Khot, K.V.; Dongale, T.; Musselman, K.P.; Bhosale, P.N. Development of dye sensitized TiO_2 thin films for efficient energy harvesting. *J. Alloys Comp.* **2019**, *790*, 1001–1013. [CrossRef]
3. Kumar, K.A.; Subalakshmi, K.; Senthilselvan, J. Effect of co-sensitization in solar exfoliated TiO_2 functionalized rGO photoanode for dye-sensitized solar cell applications. *Mater. Sci. Semicond. Process.* **2019**, *96*, 104–115. [CrossRef]
4. Tang, H.; Berger, H.; Schmid, P.E.; Lévy, F. Photoluminescence in TiO_2 anatase single crystals. *Solid State Commun.* **1993**, *87*, 847–850. [CrossRef]
5. Jauhari, H.; Grover, R.; Nanda, O.; Saxena, K. Development of quasi solid state dye sensitized solar cells. *Adv. Mater. Proc.* **2017**, *2*, 388–392. [CrossRef]
6. Asahi, R.; Morikawa, T.; Ohwaki, T.; Aoki, K.; Taga, Y. Visible-light photocatalysis in nitrogen-doped titanium oxides. *Science* **2001**, *293*, 269–271. [CrossRef] [PubMed]
7. Khan, M.M.; Ansari, S.A.; Pradhan, D.; Ansari, M.O.; Han, D.H.; Lee, J.; Cho, M.H. Band gap engineered TiO_2 nanoparticles for visible light induced photoelectrochemical and photocatalytic studies. *J. Mater. Chem. A* **2014**, *2*, 637–644. [CrossRef]
8. Ansari, S.A.; Cho, M.H. Growth of three-dimensional flower-like SnS_2 on g-C_3N_4 sheets as an efficient visible-light photocatalyst, photoelectrode, and electrochemical supercapacitance material. *Sust. Energy Fuels* **2017**, *1*, 510–519. [CrossRef]
9. Ansari, S.A.; Cho, M.H. Simple and Large Scale Construction of MoS_2-g-C_3N_4 Heterostructures Using Mechanochemistry for High Performance Electrochemical Supercapacitor and Visible Light Photocatalytic Applications. *Sci. Rep.* **2017**, *7*, 43055. [CrossRef]
10. Ansari, M.Z.; Ansari, S.A.; Parveen, N.; Cho, M.H.; Song, T. Lithium ion storage ability, supercapacitor electrode performance, and photocatalytic performance of tungsten disulfide nanosheets. *New J. Chem.* **2018**, *42*, 5859–5867. [CrossRef]
11. Ji, S.H.; Park, H.; Kim, D.; Han, D.H.; Yun, H.W.; Kim, W.B. Flexible Dye-sensitized Solar Cell Using Titanium Gel at Low Temperature. *Korean J. Mater. Res.* **2019**, *29*, 183–188. [CrossRef]
12. Holliman, P.J.; Connell, A.; Davies, M.; Carnie, M.; Bryant, D.; Jones, E.W. Low temperature sintering of aqueous TiO_2 colloids for flexible, co-sensitized dye-sensitized solar cells. *Mater. Lett.* **2019**, *236*, 289–291. [CrossRef]
13. Nguyen, H.H.; Gyawali, G.; Kim, T.H.; Bin Humam, S.; Lee, S.W. Blue TiO_2 polymorph: An efficient material for dye-sensitized solar cells fabricated using a low-temperature sintering process. *Prog. Nat. Sci. Mater. Inter.* **2018**, *28*, 548–553. [CrossRef]
14. Ehrmann, A.; Blachowicz, T. Recent coating materials for textile-based solar cells. *AIMS Mater. Sci.* **2019**, *6*, 234–251. [CrossRef]
15. Liu, J.; Li, Y.; Arumugam, S.; Tudor, J.; Beeby, S. Investigation of Low Temperature Processed Titanium Dioxide (TiO_2) Films for Printed Dye Sensitized Solar Cells (DSSCs) for Large Area Flexible Applications. *Mater. Today Proc.* **2018**, *5*, 13846–13854. [CrossRef]
16. Yun, M.J.; Cha, S.I.; Seo, S.H.; Kim, H.S.; Lee, D.Y. Insertion of Dye-Sensitized Solar Cells in Textiles using a Conventional Weaving Process. *Sci. Rep.* **2015**, *5*, 11022. [CrossRef]
17. Yun, M.J.; Cha, S.I.; Seo, S.H.; Lee, D.Y. Highly Flexible Dye-sensitized Solar Cells Produced by Sewing Textile Electrodes on Cloth. *Sci. Rep.* **2014**, *4*, 5322. [CrossRef]
18. Herrmann, A.; Fiedler, J.; Ehrmann, A.; Grethe, T.; Schwarz-Pfeiffer, A.; Blachowicz, T. Examination of the sintering process dependent micro- and nanostructure of TiO_2 on textile substrates. *Proc. SPIE* **2016**, *9898*, 98980S.

19. Juhász Junger, I.; Homburg, S.V.; Grethe, T.; Herrmann, A.; Fiedler, J.; Schwarz-Pfeiffer, A.; Blachowicz, T.; Ehrmann, A. Examination of the sintering process dependent properties of TiO_2 on glass and textile substrates. *J. Phot. Energy* **2017**, *7*, 015001. [CrossRef]
20. Greiner, A.; Wendorff, J.H. Electrospinning: A fascinating method for the preparation of ultrathin fibers. *Angew. Chem. Int. Ed.* **2007**, *46*, 5670–5703. [CrossRef]
21. Yalcinkaya, F. A review on advanced nanofiber technology for membrane distillation. *J. Eng. Fiber. Fabr.* **2019**, *14*, 1558925018824901. [CrossRef]
22. Mamun, A. Review of Possible Applications of Nanofibrous Mats for Wound Dressings. *Tekstilec* **2019**, *62*, 89–100. [CrossRef]
23. Seon-Lutz, M.; Couffin, A.C.; Vignoud, S.; Schlatter, G.; Hebraud, A. Electrospinning in water and in-situ crosslinking of hyaluronic acid/cyclodextrin nanofibers: Towards wound dressing with controlled drug release. *Carbohydr. Polym.* **2019**, *207*, 276–287. [CrossRef] [PubMed]
24. Grothe, T.; Wehlage, D.; Böhm, T.; Remche, A.; Ehrmann, A. Needleless Electrospinning of PAN Nanofibre Mats. *Tekstilec* **2017**, *60*, 290–295. [CrossRef]
25. Banitaba, S.N.; Semnani, D.; Rezaei, B.; Ensafi, A.A. Evaluating the electrochemical properties of PEO-based nanofibrous electrolytes incorporated with TiO_2 nanofiller applicable in lithium-ion batteries. *Polym. Adv. Technol.* **2019**, *30*, 1234–1242. [CrossRef]
26. Döpke, C.; Grothe, T.; Steblinski, P.; Klöcker, M.; Sabantina, L.; Kosmalska, D.; Blachowicz, T.; Ehrmann, A. Magnetic nanofiber mats for data storage and transfer. *Nanomaterials* **2019**, *9*, 92. [CrossRef] [PubMed]
27. Andre, R.S.; Mercante, L.A.; Facure, M.H.M.; Mattoso, L.H.C.; Correa, D.S. Enhanced and selective ammonia detection using In_2O_3/reduced graphene oxide hybrid nanofibers. *Appl. Surf. Sci.* **2019**, *473*, 133–140. [CrossRef]
28. García-Mateos, F.J.; Ruiz-Rosas, R.; Rosas, J.J.; Rodríguez-Mirasol, J.; Cordero, T. Controlling the Composition, Morphology, Porosity, and Surface Chemistry of Lignin-Based Electrospun Carbon Materials. *Front. Mater.* **2019**, *6*, 114. [CrossRef]
29. Heo, Y.J.; Lee, H.I.; Lee, J.W.; Park, M.; Rhee, K.Y.; Park, S.J. Optimization of the pore structure of PAN-based carbon fibers for enhanced supercapacitor performances via electrospinning. *Comp. Part B Eng.* **2019**, *161*, 10–17. [CrossRef]
30. Sabantina, L.; Rodriguez-Cano, M.A.; Klöcker, M.; Garcia-Mateos, F.J.; Ternero-Hidalgo, J.J.; Mamun, A.; Beermann, F.; Schwakenberg, M.; Voigt, A.L.; Rodriguez-Mirasol, J.; et al. Fixing PAN Nanofiber Mats during Stabilization for Carbonization and Creating Novel Metal/Carbon Composites. *Polymers* **2018**, *10*, 735. [CrossRef]
31. Juhász Junger, I.; Wehlage, D.; Böttjer, R.; Grothe, T.; Juhász, L.; Grassmann, C.; Blachowicz, T.; Ehrmann, A. Dye-sensitized solar cells with electrospun nanofiber mat-based counter electrodes. *Materials* **2018**, *11*, 1604. [CrossRef]
32. Fröse, A.; Schmidtke, K.; Sukmann, T.; Juhász Junger, I.; Ehrmann, A. Application of natural dyes on diverse textile materials. *Optik* **2019**, *181*, 215–219. [CrossRef]
33. Kohn, S.; Großerhode, C.; Storck, J.L.; Grötsch, G.; Cornelißen, C.; Streitenberger, A.; Grassmann, C.; Schwarz-Pfeiffer, A.; Ehrmann, A. Commercially available teas as possible dyes for dye-sensitized solar cells. *Optik* **2019**, *185*, 178–182. [CrossRef]
34. Ehrmann, A.; Blachowicz, T. Comment on 'Dye-sensitized solar cells using Aloe Vera and Cladode of Cactus extracts as natural sensitizers' [Chem. Phys. Lett. 679 (2017) 97–101]. *Chem. Phys. Lett.* **2019**, *714*, 227–229. [CrossRef]
35. Zheng, H.D.; Tachibana, Y.; Kalantar-zadeh, K. Dye-Sensitized Solar Cells Based on WO_3. *Langmuir* **2010**, *26*, 19148–19152. [CrossRef]
36. Sayama, K.; Sugihara, H.; Arakawa, H. Photoelectrochemical Properties of a Porous Nb_2O_5 Electrode Sensitized by a Ruthenium Dye. *Chem. Mater.* **1998**, *10*, 3825–3832. [CrossRef]